

PII: S0017-9310(97)00143-9

Heat transfer correlations for small, uniformly heated liquid pools

MOHAMED S. EL-GENK and HAMED H. SABER

Institute for Space and Nuclear Power Studies/Chemical and Nuclear Engineering, University of New Mexico, Albuquerque, NM 87131-1341, U.S.A.

(Received 20 December 1996 and in final form 14 May 1997)

Abstract—Heat transfer data of numerous investigators for uniformly-heated liquid pools of water, ethanol, methanol, Dowtherm-A, R-11 and R-113 in small cylindrical enclosures were compiled, sorted, and correlated in the following heat transfer regimes: (a) natural convection; (b) nucleate boiling; and (c) combined convection. In the combined convection, where both natural convection and nucleate boiling contribute to the heat transfer, the data were correlated by superimposing the natural convection and nucleate boiling heat transfer correlations using a power law approach as:

$$Nu_{CC} = (Nu_{NC}^4 + Nu_{NB}^4)^{0.25}$$

All correlations were within $\pm 15\%$ of most experimental data. The data covered a wide range of pool diameters (6–37 mm), heated pool heights (50–800 mm), working fluid filling ratios (0.1–3.25), and wall heat fluxes (0.7–383 kW m⁻²). © 1997 Elsevier Science Ltd.

INTRODUCTION

Heat transfer regimes in uniformly heated liquid pools in small cylindrical enclosures, similar to those in the evaporator of enclosed, gravity-assisted, two-phase thermosyphons (GATPT), are of interest in many industrial and energy applications. Examples of these applications include oil refineries; fragrance, cosmetic, chemical, and pharmaceutical industries; geothermal energy recovery; and gas-gas and gas-liquid thermosyphon heat exchangers in metals, glass, and other smoke stack industries with high energy utilization. Several heat transfer regimes are encountered in small, enclosed liquid pools, depending on the wall heat flux, the vapor pressure or temperature, the liquid physical properties, and the inner diameter of the pool. Natural convection, is the dominant mode of heat transfer in the pool at low heat fluxes [Fig. 1(a)]. In this regime, limited nucleation at the wall also contributes to the heat transfer from the wall to the liquid pool by thermosyphon effect, whereas evaporation and condensation of the working fluid occur at the base and top of the bubbles, respectively. In addition, the hot liquid next to the wall rises to the pool surface and is replaced by a cooler liquid that flows down near the center of the pool under the effect of gravity. This heat transfer regime at GATPTs has received little attention; natural convection data were either ignored or inadvertently incorporated in the data base for the combined convection [Fig. 1(b)] and the nucleate boiling [Fig. 1(c)] regimes.

The combined convection regime, which has also been referred to by some investigators as two-phase convection regime, occurs at intermediate wall heat

fluxes, where both natural convection and nucleate boiling contribute to the heat transfer in the pool. In this regime, the nucleation and growth of bubbles at the wall, as well as the induced mixing by the sliding bubbles along the wall effectively enhance the heat transfer coefficient.

At high wall heat fluxes, the heat transfer in small, enclosed liquid pools occurs by nucleate boiling [Fig. 1(c)]. In this regime, conventional boiling heat transfer correlations are not directly applicable [1–4] because they do not account for the effect of mixing along the heated wall by sliding bubbles and in the pool by departing and rising bubbles [Fig. 1(c)]. When the bubbles reach the pool surface they burst dispersing tiny liquid droplets into the vapor flow above the liquid pool, which also enhance the nucleate boiling heat transfer in small, enclosed liquid pools.

Owing to the complexity of heat transfer in small liquid pools, only empirical and semi-empirical correlations have been reported [5–11]. Most reported correlations, however, have exhibited large discrepancies with the experimental data, ranging from –70 to +400% in some cases. The first attempt to compile and sort the heat transfer data of various investigators was that of Groß [10]. He neglected the natural convection regime, and sorted and correlated the data in what he called the two-phase convection regime and in the nucleate boiling regime. His correlations showed discrepancies ranging from –30% to +70% with experimental data. Therefore, there is a need to re-examine the reported heat transfer data for liquid pools in small, enclosures, such as in GATPTs, and to develop more accurate heat transfer correlations.

NOMENCLATURE

Ar	Archimid number, $(gd_i^3/v_i^2)((\rho_l - \rho_g)/\rho_l)$, equation (1)	Ra	Rayleigh number $(\beta g d_i^4 q_e / k_i \alpha_i \nu_i)$, equation (10)
Bo	Bond number, $d_i / \sqrt{\sigma / (g(\rho_l - \rho_g))}$	T	temperature [K]
C_p	specific heat [J kg ⁻¹ K ⁻¹]	X	dimensionless pool parameter, equation (14).
C_{sf}	coefficient, equation (6)		
d	diameter [m]		
Fr	Froude number, $(q_e / \rho_l h_{fg})^2 (\rho_l / d_i g (\rho_l - \rho_g))$, equation (1)	Greek symbols	
g	gravitational acceleration [m s ⁻²]	α	thermal diffusivity [m ² s ⁻¹]
h	heat transfer coefficient [W m ⁻² K]	β	thermal expansion coefficient (K ⁻¹)
h_{fg}	latent heat of vaporization [J kg ⁻¹]	l_m	bubble length scale, $(\sigma / (g(\rho_l - \rho_g)))^{0.5}$ [m]
h_{Ku}	Kutatelatze's nucleate boiling heat transfer coefficient [W m ⁻² K ⁻¹], equation (8)	μ	dynamic viscosity [N. s m ⁻²]
k	thermal conductivity [W m ⁻¹ K ⁻¹]	ν	kinematic viscosity [m ² s ⁻¹]
L	length [m]	ρ	density [kg m ⁻³]
M	molecular weight [kg kmol ⁻¹]	σ	surface tension [N m ⁻¹]
n	exponent, equations (1)–(2)	ψ	mixing coefficient, equation (12).
Nu	Nusselt number (hd_i/k_i)	Subscripts	
Nu_{Ku}	Kutatelatze's Nusselt number $(h_{Ku} l_m / k_i)$	bp	expanded boiling pool
P	pressure [Pa]	c	critical, condenser
P_a	atmospheric pressure (1.013×10^5 Pa)	CC	combined convection
p_c	critical pressure [Pa]	e	evaporator
p_r	reduced pressure (p/p_c)	g, v	vapor
Pr	Prandtl number	i	inner
q	heat flux [W m ⁻²]	l	liquid
Q	power throughput [w]	NB	nucleate boiling
R	surface roughness [μ m], equation (7)	NC	natural convection
		p	liquid pool
		TC	two phase convection.

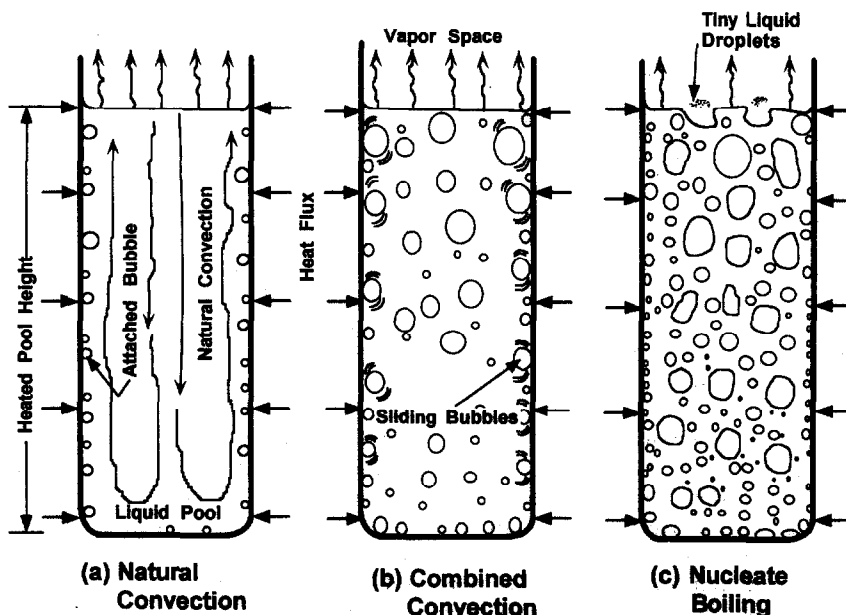


Fig. 1. A schematic of different heat transfer regimes in uniformly heated, small liquid pools.

In this paper, a total of 731 heat transfer data points of numerous investigators for water, ethanol, methanol, Dowtherm-A, R-11, R-113, were compiled, carefully examined, and sorted into the appropriate heat transfer regimes. The data covered a wide range of pool diameters (6–37 mm), heated pool height (50–800 mm), working fluid filling ratios (0.1–3.25), and wall heat fluxes (0.7–383 kW m⁻²). The natural convection and nucleate pool boiling data were correlated separately using the appropriate dimensionless variables for each regime. In the combined convection regime, since both natural convection and nucleate boiling contribute to the heat transfer, the data were correlated by superimposing the correlations of natural convection and nucleate boiling using a power law approach [12, 14–17], to ensure a continuous and smooth transition among all three heat transfer regimes.

PREVIOUS HEAT TRANSFER CORRELATIONS

As indicated earlier, the three heat transfer regimes which occur in small liquid pools in cylindrical enclosures are: (a) *natural convection*, at low heat fluxes (b) *combined convection*, at intermediate heat fluxes and (c) *nucleate boiling*, at high heat fluxes (Fig. 1). This section reviews heat transfer correlations reported by various investigators in these heat transfer regimes.

Natural convection

Because of its relatively low heat transfer coefficient, natural convection in small, enclosed liquid pools has received very little attention [10]. Natural convection data were either neglected [10], or inadvertently incorporated into the data base of the two-phase convection and the nucleate boiling regimes [6, 7]. Therefore, there have been no correlations reported for natural convection in the small liquid pools in GATPTs.

Combined convection

In the combined convection regime, in addition to natural convection, bubble nucleation occurs at selected sites on the heated wall. The departing vapor bubbles slide and rise along the wall separated by a thin stationary liquid layer [Fig. 1(b)]. These bubbles grow in size by evaporation at the interface between the thin liquid layer and the rising bubbles. The efficient heat conduction in the thin liquid layer separating the sliding bubbles from the heated wall and the mixing and agitation induced by the rising bubbles in the pool, greatly enhance the heat transfer in the combined convection regime [Fig. 1(b)]. Thus, combined convection is basically a transition regime between *natural convection*, where the heat transfer coefficient increases with the wall heat flux raised to the power 0.25 to 0.35, and *nucleate boiling*, where the heat transfer coefficient increases with the wall heat flux raised to the power 0.67 to 0.7.

Recently, Groß [10] compiled an extensive data

base of 2529 experimental points for a wide range of working fluids, pool dimensions, vapor pressures, and wall heat fluxes. He used the data to develop two empirical heat transfer correlations for two-phase convection and nucleate boiling. His two-phase convection correlation was given as:

$$h_{TC} = 4.0(k_l/d_i)(Ar Fr^{0.5})^{1/3} Pr_l^{0.5} (Bo/10)^n \quad (1)$$

where $n = 0.5$ for $Bo \leq 10$ and $n = 1/6$ for $Bo > 10$. This correlation predicted most of the experimental data classified in this regime by Groß [10], to within $\pm 30\%$ (Fig. 2), but in some cases it deviated from the data by more than $\pm 50\%$ [10]. When expanded to show the dependence of the heat transfer coefficient on the wall heat flux, equation (1) reads [10]:

$$h_{TC} = (4.0/10^n) q_c^{1/3} (k_l^{0.5} C p_l^{0.5} \rho_l^{1/6} d_i^{(n-1/6)} / (\mu_l^{1/6} \sigma^{0.5n} h_{fg}^{1/3})) ((\rho_l - \rho_g) g)^{(0.5n+1/6)}. \quad (2)$$

Equation (2) indicates that the heat transfer coefficient increases with increasing evaporator heat flux raised to 1/3 power, suggesting that the data on which equation (2) was based actually belongs for the most part in the natural convection regime, which Groß [10] neglected.

Nucleate boiling

In the nucleate boiling regime, Imura *et al.* [6] proposed a correlation by multiplying that of Kusuda and Imura [5], for open thermosyphons, with a pressure correction factor, $[1.2 (P/P_a)^{0.3}]$, determined from the least-square fit of their experimental data for water and ethanol. The nucleate boiling correlation of Imura *et al.* [6] was given as:

$$h_{NB} = 0.32 q_c^{0.4} \left(\frac{\rho_l^{0.65} k_l^{0.3} C p_l^{0.7} g^{0.2}}{\rho_g^{0.25} h_{fg}^{0.4} \mu_l^{0.1}} \right) (p/p_a)^{0.3}. \quad (3)$$

In this correlation, since the exponent of the wall heat flux is only 0.4, it could be argued that the heat transfer data of Imura *et al.* [6] do not entirely belong in the nucleate boiling regime. As shown in Table 1, the water and ethanol data of Imura *et al.* [6] spanned all three regimes of natural convection, combined convection, and nucleate boiling.

Shiraishi *et al.* [7] correlated their heat transfer data for water, ethanol, and R-113 using equation (3), after changing the exponent of the pressure term on the right hand from 0.3 to 0.23. Such a change was based on a least-square fit of their own experimental data. In the experiments, the vapor temperatures were 305, 318 and 333 K for water, 305 and 318 K for ethanol, and 305 K for R-113 and the working fluids filling ratios were 0.5 and 1.0. Shiraishi *et al.* [7] determined the average heat transfer coefficient in the pool based on the wall heat flux and the mean temperature difference between the wall and the pool and correlated the data as:

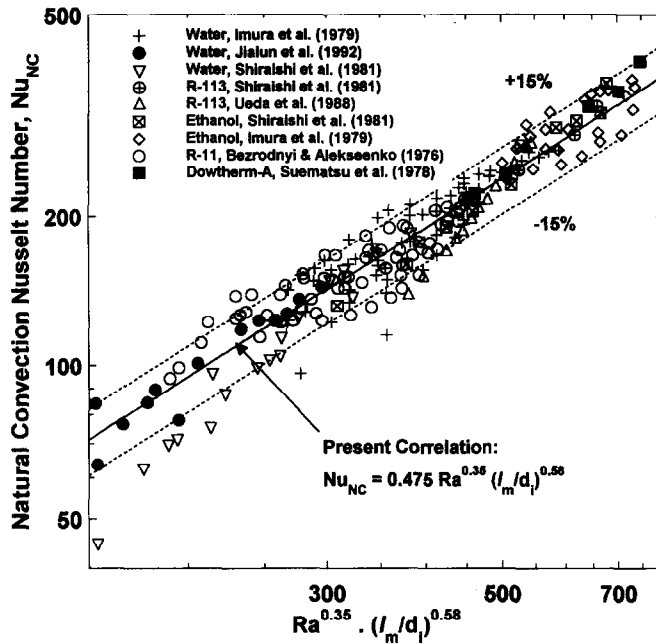


Fig. 2. Comparison of present natural convection correlation [equation (10)] with data.

$$h_{NB} = 0.32q_e^{0.4} \left(\frac{\rho_1^{0.65} k_1^{0.3} C p_1^{0.7} g^{0.2}}{\rho_g^{0.25} h_{fg}^{0.4} \mu_1^{0.1}} \right) (p/p_a)^{0.23}. \quad (4)$$

This equation, however, is consistently lower than the ethanol data of Shiraishi *et al.* [7] by more than 30%, about 12% higher than the R-113 data, and more than 30% higher than the water data at low heat transfer coefficients ($< 2000 \text{ W m}^{-2} \text{ K}^{-1}$), but within $\pm 10\%$ of the data at high heat transfer coefficients ($> 4500 \text{ W m}^{-2} \text{ K}^{-1}$). Equation (4) shows that the heat transfer coefficient increases with increasing wall heat flux raised to 0.4 power, instead of 0.67–0.7 as would be expected in the nucleate pool boiling regime [1–3]. The small exponent suggests that the data of Shiraishi *et al.* [7] do not belong in the nucleate boiling regime. Actually, the water, R-113 and most of the ethanol data of Shiraishi *et al.* belong in the natural convection and combined convection regimes, and only a few data points for R-113 belong in the nucleate boiling regime (Table 1).

To correlate the data that he compiled and classified in the nucleate boiling regime, Groß [10] modified Cooper's correlation [13], developed originally for general purpose nucleate boiling, by substituting 1.0 μm for the roughness parameter and using an exponent of 0.7 instead of 0.67 for the wall heat flux as:

$$h_{NB} = 55q_e^{0.7} (p_r^{0.12} / ((-\log_{10} p_r)^{0.55} \sqrt{M})). \quad (5)$$

Ueda *et al.* [8] modified Roshenow's correlation for nucleate pool boiling [3] to fit their own data for water, methanol and R-113, as:

$$h_{NB} = C_{sf}^{-1} Pr^{-1.7} (C p_1 q_e / h_{fg}) (q_e l_m / (\mu_1 h_{fg}))^{-1/3}. \quad (6)$$

They kept the exponent of Prandtl number for all

three working fluids the same as in Roshenow's correlation (–1.7), but obtained different values of the coefficient C_{sf} for the different working fluids (0.0098 for water, 0.0028 for methanol, and 0.0047 for R-113), based on the least-square best fits of the data.

Kaminaga *et al.* [9] performed heat transfer experiments using water, R-113, and ethanol and covered a wide range of wall heat fluxes, vapor pressures, and filling ratios (Table 1). The inner surface of the wall had a roughness, $R = 0.53 \mu\text{m}$. They correlated their nucleate boiling heat transfer data, in terms of that of Kutatelatze's [2] for conventional pool boiling, as:

$$h_{NB} = 22(\rho_g/\rho_1)^{0.4} R^{0.2(1-P_r)} h_{Ku}. \quad (7)$$

The nucleate boiling heat transfer coefficient correlation of Kutatelatze [2], h_{Ku} , is:

$$h_{Ku} = 6.95 \times 10^{-4} (k_1/l_m) Pr_1^{0.35} (q_e l_m / (\rho_g h_{fg} v_1))^{0.7} (Pl_m/\sigma)^{0.7}. \quad (8)$$

Equation (7) agreed with the experimental data of Kaminaga *et al.* [9] for ethanol to within $\pm 20\%$ and with most of the water and R-113 data to within ± 20 and $\pm 30\%$, respectively. At low heat flux, the experimental heat transfer coefficients of Kaminaga *et al.* [9] for water and R-113 were significantly higher than predicted by equation (7), suggesting that their low heat flux data for these two fluids do not actually belong in the nucleate boiling, but rather in the combined convection regime, as shown in Table 1. When the data of Kaminaga *et al.* [9] were compared to Groß's [10] correlation [equation (5)], there was a large discrepancy, ranging from –45 to +70%.

Jialun *et al.* [11] proposed the following correlation for the average heat transfer coefficient in the pool, in

Table 1. Compiled heat transfer data for small, uniformly heated liquid pools in cylindrical enclosures

Regime	Reference	Data points	Working fluid	L_e [mm]	d_i [mm]	T_v [K]	q_e [kW m ⁻²]
Natural convection	Bezrodyi and Alekseenko [18]	59	R-11	50–800	8–12	296	2.31–9.53
	Ueda <i>et al.</i>	13	R-113	115	14.8	277–285	10–18
	Shiraishi <i>et al.</i>	4	R-113	280	37	305	1.02–8
	Shiraishi <i>et al.</i>	13	Ethanol	280	37	305–318	0.7–8.7
	Imura <i>et al.</i>	23	Ethanol	300	28	302–340	11.2–33.9
	Shiraishi <i>et al.</i>	14	Water	280	37	305–333	1.7–14.7
	Imura <i>et al.</i>	66	Water	100–300	28	298–363	11.1–45
	Jialun <i>et al.</i>	13	Water	700	19.6	375	5–25
	Suematsu	3	Dowtherm-A	250	16.7	533–613	4–9.4
	Combined convection	Bezrodyi and Alekseenko [18]	27	R-11	50–800	8–12	296
Ueda <i>et al.</i>		13	R-113	115	14.8	280–292	18–27
Shiraishi <i>et al.</i>		4	R-113	280	37	305	8–10
Kaminaga <i>et al.</i>		12	R-113	431	19.5	300–318	2.9–3.75
Shiraishi <i>et al.</i>		12	Ethanol	280	37	305–318	7.7–35
Imura <i>et al.</i>		19	Ethanol	300	28	323–349	22.5–33.9
Kaminaga <i>et al.</i>		13	Ethanol	431	19.5	315–353	8.9–28.1
Shiraishi <i>et al.</i>		20	Water	280	37	305–333	9.6–39.7
Imura <i>et al.</i>		48	Water	100–300	28	315–378	33.8–90.5
Jialun <i>et al.</i>		8	Water	700	19.6	375	25–46
Kaminaga <i>et al.</i>		8	Water	431	19.5	319–343	19–35
Ueda <i>et al.</i>		5	Water	115	14.8	363–367	83.7–105
Suematsu		7	Dowtherm-A	250	16.7	533–613	9.5–23.9
Nucleate boiling	Bezrodyi and Alekseenko [18]	32	R-11	50–800	8–12	296	15.4–68.4
	Fujii	10	R-11	300	17	343	11.7–48.4
	Shiraishi <i>et al.</i>	5	R-113	280	37	305	10–37.7
	Kaminaga <i>et al.</i>	23	R-113	431	19.5	317–372	3.6–39.4
	Imura <i>et al.</i>	11	Ethanol	300	28	342–367	33.9–56.4
	Kaminaga <i>et al.</i>	22	Ethanol	431	19.5	353–446	28.1–116
	Ueda <i>et al.</i>	23	Methanol	115	14.8	326–340	27–60
	Bezrodyi and Alekseenko [22]	6	Methanol	200–400	20	339	32–56
	Bezrodyi and Alekseenko [18]	97	Water	50–800	6–12	318–450	40–150
	Imura <i>et al.</i>	5	Water	100–300	28	374–379	90.2–90.5
	Xin <i>et al.</i>	30	Water	475	20	366–448	25–45
	Kaminaga <i>et al.</i>	32	Water	431	19.5	341–497	27.3–383
	Ueda <i>et al.</i>	21	Water	115	14.8	365–373	90.4–155
	Suematsu	10	Dowtherm-A	250	16.7	533–613	19–69.6

terms of the measured expanded liquid pool height in their experiments (L_{bp}) as:

$$h_p = 14.45 \left(\frac{k_l}{d_i} \right) \left(\frac{d_i q_e}{h_{fg} \mu_l} \right)^{0.39} Pr_l^{0.75} \left(\frac{L_{bp}}{d_i} \right)^{0.12} \left(\frac{\rho_l}{\rho_g} \right)^{0.2} \quad (9)$$

Equation (9) is developed solely based on the authors' own data for water, ethanol and acetone and agreed with the data for all three liquids, to within $\pm 20\%$. The exponent of the wall heat flux is 0.39, however, suggesting that the data do not actually belong in the nucleate boiling regime. When compared with the correlations of other investigators, equation (9) was $\sim 15\%$ lower than the correlation of Shiraishi *et al.* [7] for nucleate boiling, equation (4), 30% lower than the two-phase convection correlation of Groß [10], equation (2), and about five times higher than the nucleate boiling correlation of Cooper [13] at low heat

flux (1.0 kW m⁻²). The difference between Groß's correlation, equation (2), and the data of Jialun *et al.* [11] decreases with increasing wall heat flux, reaching about 20% at 100 kW m⁻². In the following section, the heat transfer data of various investigators for different working fluids, dimensions and operating conditions, were sorted and correlated in the appropriate heat transfer regime (Table 1).

PRESENT HEAT TRANSFER CORRELATIONS

A total of 731 experimental data points of numerous investigators for uniformly heated, small liquid pools of water, ethanol, methanol, Dowtherm-A, R-11 and R-113 in cylindrical enclosures were compiled. The data cover a wide range of pool dimensions and operating conditions (Table 1). The classification of the data in the different heat transfer regimes, namely: natural convection, combined convection and

nucleate boiling, was based on the exponent of the wall heat flux that best correlated the data. The data that showed a dependence of the heat transfer coefficient or Nusselt number on the wall heat flux raised to the 0.67–0.7 power, were classified in the nucleate boiling regime, while those showing a dependence on the wall heat flux raised to a power of 0.25–0.35 were classified in the natural convection regime. The rest of the data, for which exponent of the wall heat flux ranges from 0.35 to 0.67, were classified in the intermediate regime of combined convection.

The data in the natural convection and the nucleate boiling regimes were correlated separately using appropriate dimensionless parameters, which collapse the data of the different working fluids in the same heat transfer regime. The two correlations were then superimposed using a power law approach, to correlate the data for the intermediate regime of combined convection and ensure smooth transition between these regimes. This approach has been successfully applied to correlating combined convection data in vertical pipes, annuli and rod-bundles [12, 14–17]. However, to the best of our knowledge, the validity of this approach to combined convection in small liquid pools in cylindrical enclosures has never been examined before this work. The success of this approach depends not only on the proper sorting of the data, but also on the selection of the appropriate dimensionless parameters to correlate the data in the natural convection and the nucleate boiling regimes.

Natural convection correlation

A total of 208 experimental data points were identified and used to develop the present natural convection correlation (Table 1). In this regime, although

heat transfer to the liquid pool from the uniformly heated wall is dominated by natural convection, limited bubble nucleation on the bottom and along the heated wall also contributes to the heat transfer in the pool [Fig. 1(a)]. In order to account for these effects, Nusselt number data for natural convection were correlated in terms of the liquid Rayleigh number and the ratio of the bubble length scale, l_m , to the inner diameter of the pool, d_i , as

$$Nu_{NC} = 0.475 Ra^{0.35} (l_m/d_i)^{0.58}. \quad (10)$$

As shown in Fig. 2, equation (10) is in good agreement with most of the data for water, ethanol, R-11, R-113 and Dowtherm-A, to within $\pm 15\%$. When the second term on the right-hand side of equation (10) was removed, there was a large scattering among the data of the different working fluids, confirming the important contribution of bubble nucleation to natural convection heat transfer in small liquid pools, which increases with decreasing pool diameter.

When the same data in Fig. 2, were compared to the two-phase convection correlation of Groß [10], equation (2), in which the wall heat flux has an exponent of $1/3$ vs 0.35 for Ra in equation (10), there was a large scattering among the data of the different working fluids. Also, as shown in Fig. 3, the deviation between equation (2) and the data is as much as $\pm 30\%$.

Nucleate boiling correlation

A total of 327 data points for water, methanol, ethanol, Dowtherm, R-113 and R-11 were confirmed in the nucleate boiling regime (Table 1). These data were correlated in terms of the Nusselt number of

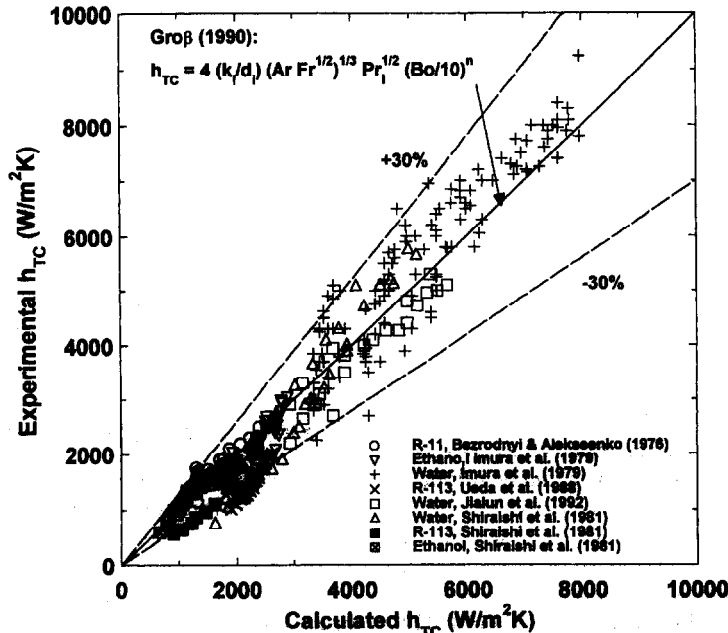


Fig. 3. Comparison of Groß's correlation for two-phase convection [equation (2)] with natural convection data.

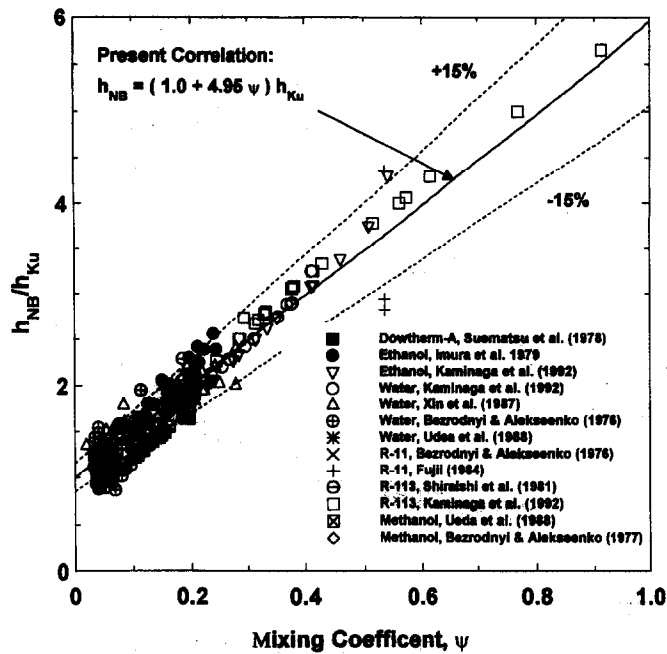


Fig. 4. Comparison of present nucleate boiling correlation [equation (11)] with data.

Kutatelatze [2], Nu_{Ku} , for conventional nucleate pool boiling, after accounting for the effect of mixing in the boundary layer by sliding bubbles along the wall and in the pool by departing and rising bubbles, as:

$$Nu_{NB}(l_m/d_i) = (1.0 + 4.95\psi)Nu_{Ku} \quad (11)$$

where,

$$\psi = (\rho_g/\rho_l)^{0.4} ((pv_l/\sigma)(\rho_l^2/(\sigma g(\rho_l - \rho_g))))^{0.25} \quad (12a)$$

Equation (11) can be written for the nucleate boiling heat transfer as:

$$h_{NB} = (1.0 + 4.95\psi)h_{Ku} \quad (12b)$$

The mixing coefficient, ψ , in equation (11) reflects for the contribution of mixing by sliding and rising bubbles to the nucleate boiling heat transfer in small liquid pools. As delineated in Fig. 4, equation (11) is in good agreement with most of the nucleate pool boiling data of the different working fluids, to within $\pm 15\%$; this agreement could have been better had it not been for the reported large scattering in the water data by Bezrodnyi and Alekseenko [18].

Owing to the small diameter of the pools (≤ 37 mm), bubbles nucleation and sliding of vapor bubbles along the inside of the pool wall as well as the vigorous agitation and mixing in the pool by rising large bubbles and vapor slugs, greatly enhance nucleate boiling heat transfer. As a result, the nucleate boiling heat transfer coefficient in a small liquid pool [equation (11)] could be significantly higher than that predicted by nucleate boiling correlations for conventional boiling in large open pools [equation (8)].

The mixing coefficient, ψ , which depends on the

physical properties of the working fluid, increases with increasing vapor pressure in the pool enclosure, due to increased mixing in the pool by vapor bubbles (Figs. 5 and 6). For example, decreasing the power throughput to the evaporator of an enclosed GATPT lowers the vapor pressure and increases the latent heat of vaporization, thus decreasing the vapor generation rate and the mixing in the pool by departing and rising bubbles (Fig. 6). Conversely, for the same power throughput, decreasing the inner diameter of an enclosed GATPTs, increases the vapor pressure, resulting in more mixing in the pool. Therefore, increasing the vapor pressure by either decreasing the inner diameter of the pool, or increasing the power throughput would enhance the nucleate boiling heat transfer in enclosed small liquid pools (Figs. 5 and 6).

Figures 5 and 6 plot the mixing coefficient for R-11, R-113, methanol, ethanol and water versus the vapor temperature. As Fig. 5 indicates, equation (12a) for the mixing coefficient is in excellent agreement with the data reported by various investigators. Figure 5 also shows that at the same vapor temperature, the low vapor pressure working fluids have lower mixing coefficients than high vapor pressure working fluids, which have lower latent heats of vaporization. Such low latent heats of vaporization result in higher rates of vapor generation and, hence, higher mixing coefficient (Fig. 5). The difference between the values of the mixing coefficient for the low and high vapor pressure working fluids increases with increasing vapor temperature. For example, at a vapor temperature of 350 K, the mixing coefficient for water is 0.04, while that for ethanol is about four times higher (~ 0.19), for a difference of 0.15. At a higher vapor temperature of 390 K, these coefficients increase to

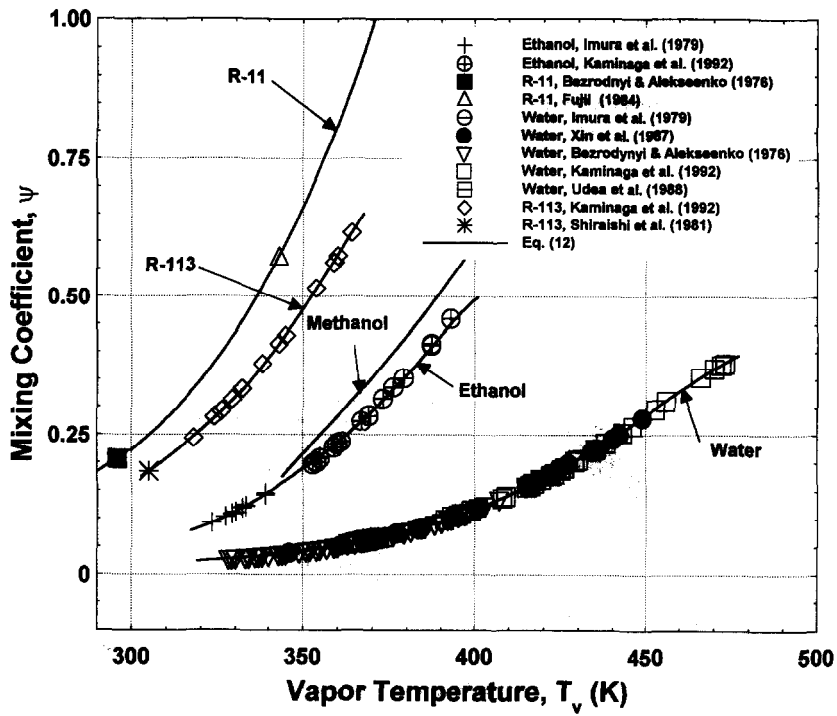


Fig. 5. Dependence of nucleate boiling mixing coefficient of different fluids on vapor temperature.

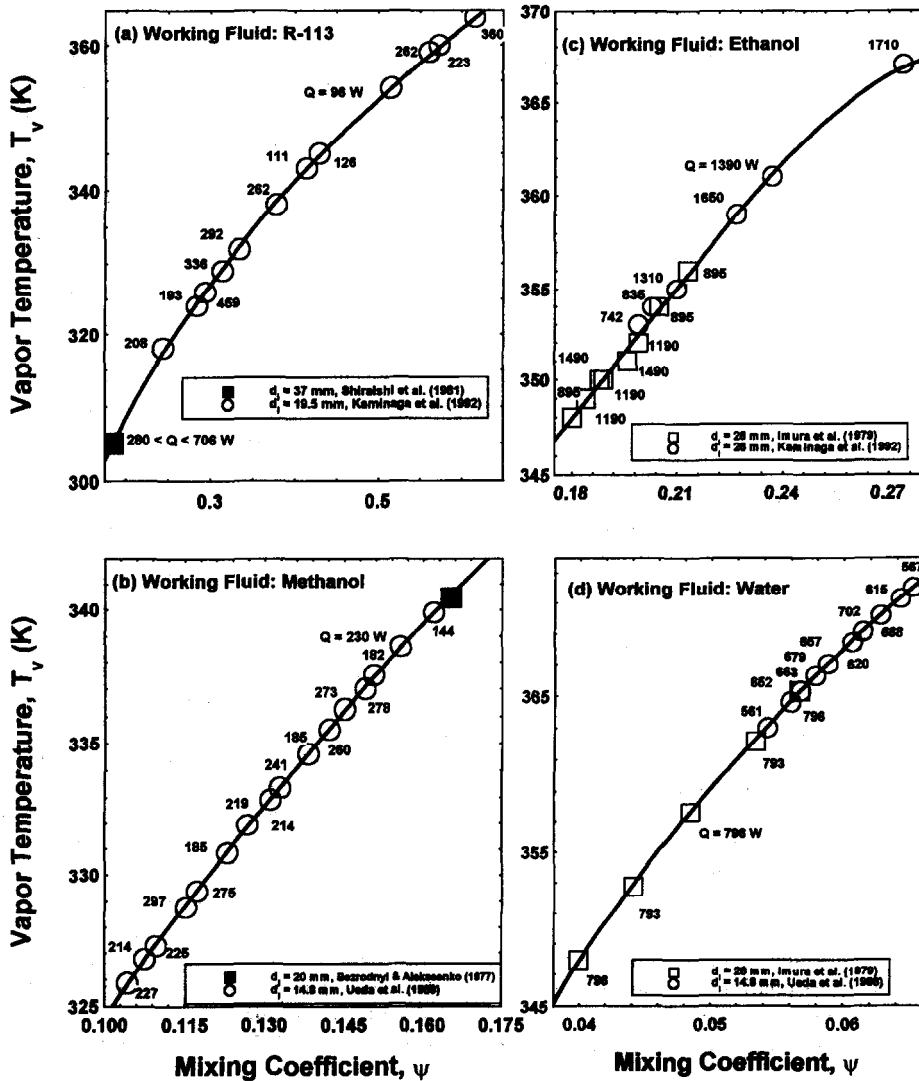


Fig. 6. Effect of power throughput and vapor temperature on nucleate boiling mixing coefficient.

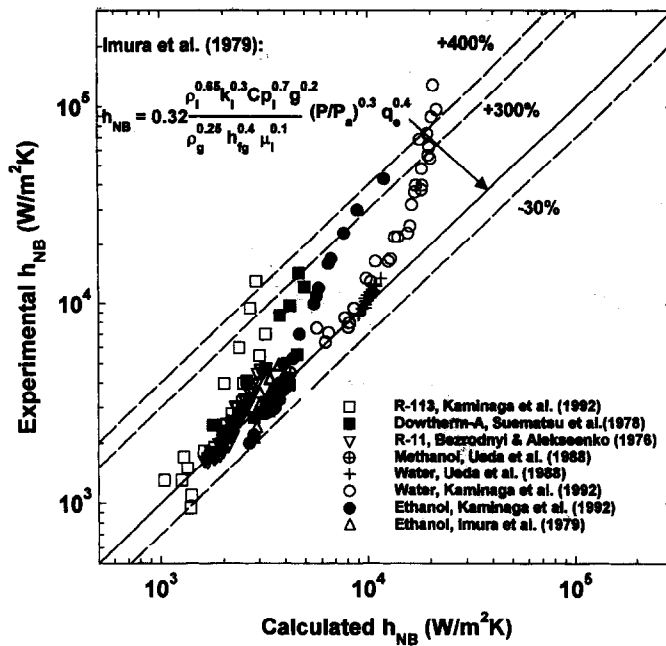


Fig. 7. Comparison of Imura *et al.*'s correlation [equation (3)] with nucleate boiling data.

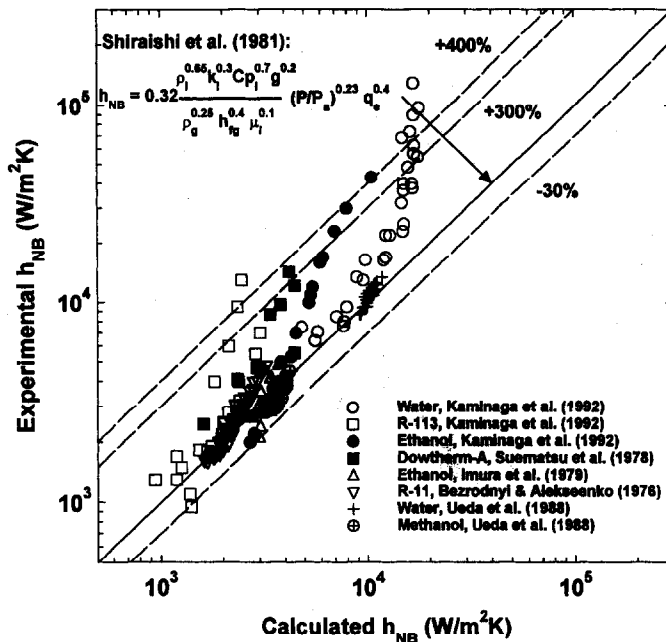


Fig. 8. Comparison of Shiraishi *et al.*'s correlation [equation (4)] with nucleate boiling data.

0.1 and 0.43 for water and ethanol, respectively, for a difference of 0.33. Figure 5 also shows that the mixing coefficient for small liquid pools decreases with decreasing vapor temperature and as it approaches zero the nucleate boiling Nusselt number in the pool becomes equal to that of Kutatelatze's. The present nucleate boiling correlation [equation (11)] suggests that the grouping of the physical parameters in Kutatelatze's correlation [equation (8)] for nucleate boiling

in large pools, are suitable for small, enclosed liquid pools.

The present nucleate boiling data are compared with the nucleate boiling correlations by other investigators in Figs 7–11 and with equation (11) in Fig. 12. Figures 7 and 8 show large discrepancies between the data and the correlations of Imura *et al.* [6], equation (3), and Shiraishi *et al.* [7], equation (4), respectively. The deviation of these correlations from the

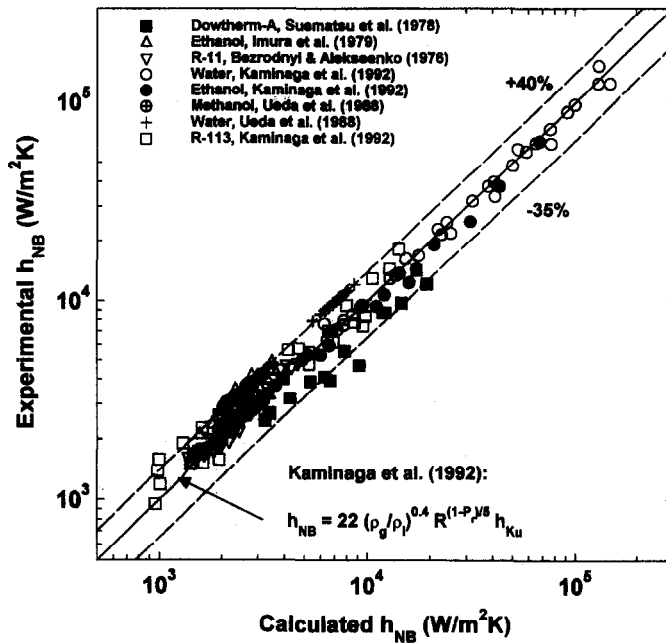


Fig. 9. Comparison of Kaminaga *et al.*'s correlation [equation (7)] with nucleate boiling data.

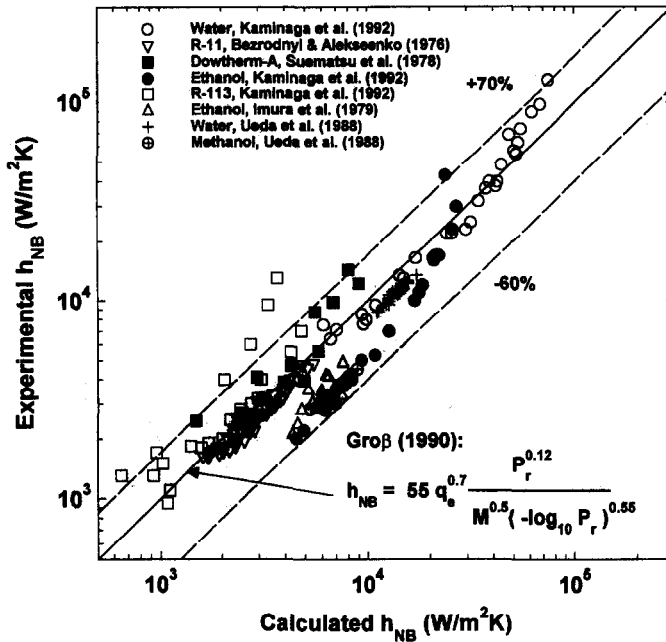


Fig. 10. Comparison of Grob's correlation [equation (5)] with nucleate boiling data.

data ranged from -30 to +400%. Furthermore, the choices of the variables in these correlations failed to properly collapse the nucleate pool boiling data of the different working fluids. The correlation of Kaminaga *et al.* [9], equation (7), agrees much better with the nucleate pool boiling data, whereas the deviation between the data and the correlation ranges from -35 to +40% (Fig. 9).

The deviation of the nucleate boiling correlation of

Grob [10], equation (5), from the present nucleate boiling data ranges from -60 to +70% (Fig. 10). Also, the choices of the parameters in Grob's correlation failed to collapse the data of the different working fluids (Fig. 10). The correlation of Ueda *et al.* [8], equation (6), compares best with the present nucleate pool boiling data for water, methanol and R-113; the deviation between the correlation and data ranges from -25 to +30% (Fig. 11). The dimen-

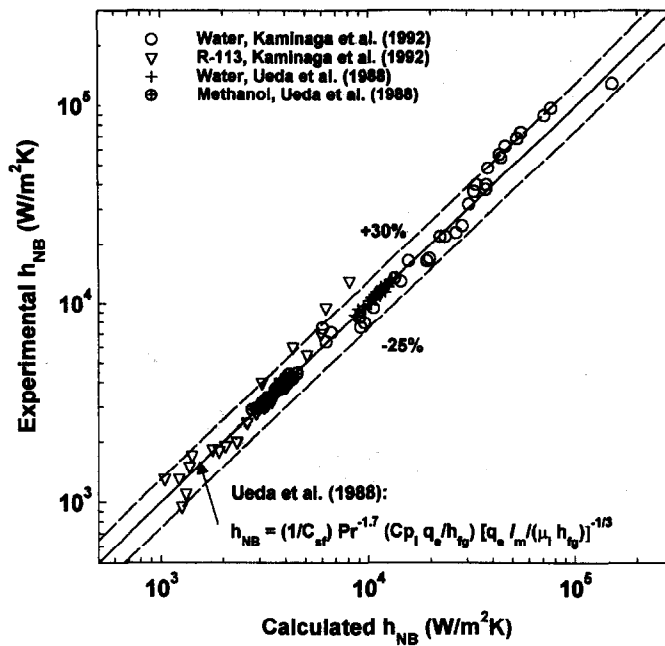


Fig. 11. Comparison of Ueda *et al.*'s correlation [equation (6)] with nucleate boiling data.

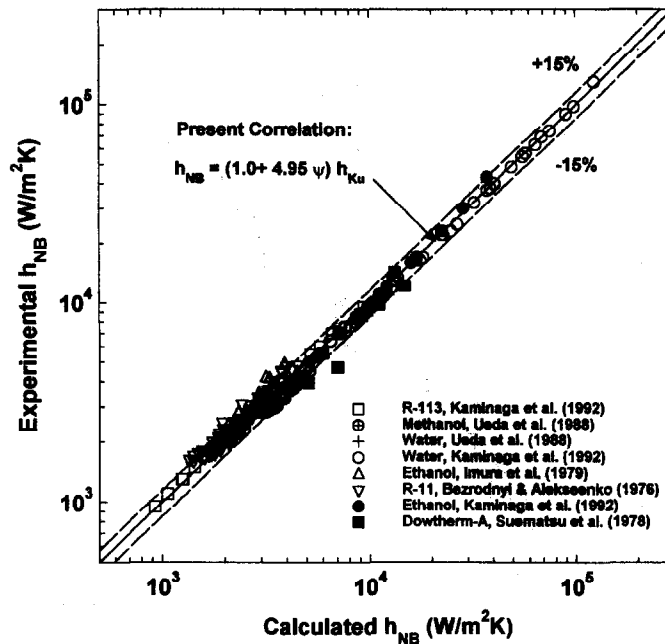


Fig. 12. Comparison of present correlation [equation (11)] with nucleate boiling data.

sionless groups in equation (6) did a good job in collapsing the data of the different working fluids.

The present nucleate boiling correlation, equation (11), did an excellent job in collapsing the data of different liquids, including water, methanol, ethanol, R-11, R-113 and Dowtherm-A, with a maximum deviation of $\pm 15\%$ between the correlation and most of the data (Fig. 12). Therefore, it is concluded that the mixing coefficient, ψ , in the present nucleate pool boiling correlation, equation (11), complements nicely the choices of the dimensionless groups in Kut-

atelatz's correlation [2], equation (8), for correlating nucleate boiling heat transfer in small, enclosed liquid pools.

Combined convection correlation

A combined convection correlation for uniformly heated, small liquid pools in cylindrical enclosures, such as in the evaporator of GATPTs, was also developed by superimposing the present correlations of natural convection [equation (10)] and nucleate

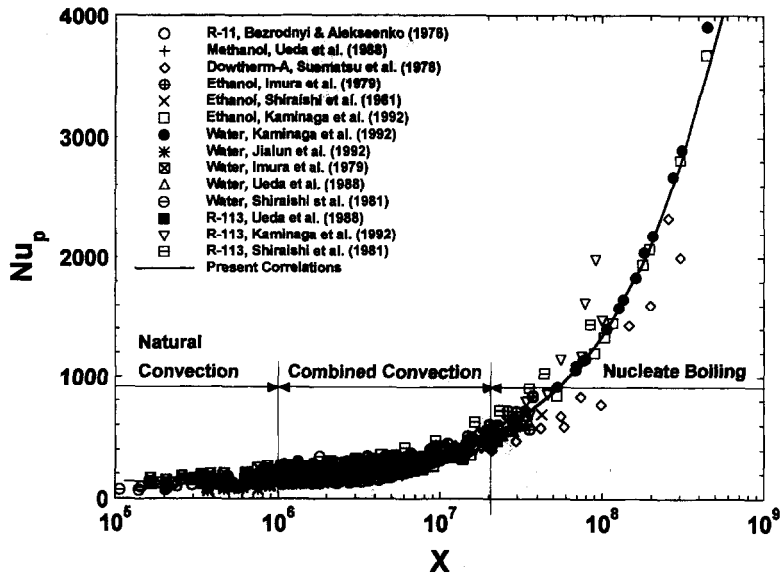


Fig. 13. Comparison of present combined convection correlation [equation (13)] with data.

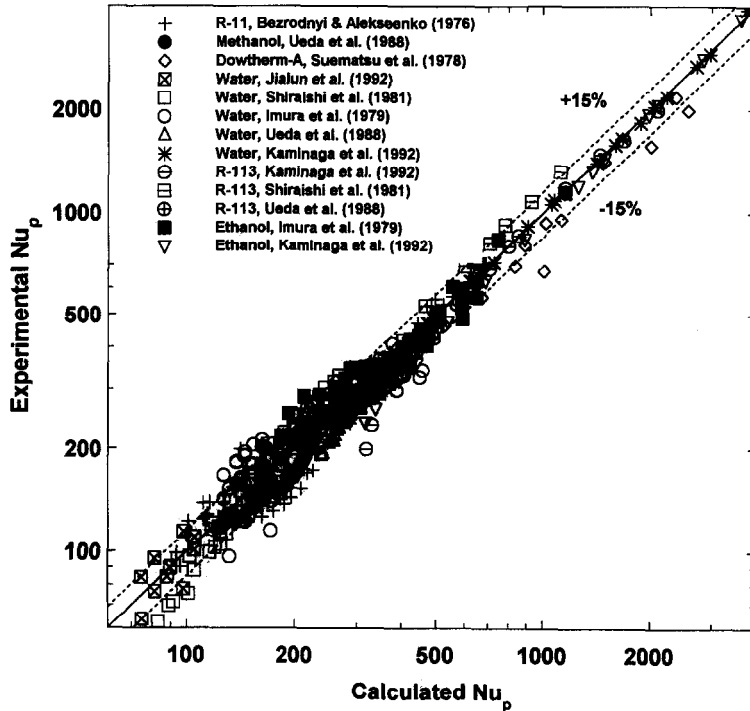


Fig. 14. Comparison of present correlations with entire heat transfer data base.

boiling [equation (11)] using a power law approach [12, 14–17] as:

$$Nu_{CC} = (Nu_{NC}^4 + Nu_{NB}^4)^{0.25} \tag{13}$$

Equation (13) is in a good agreement with the data in the combined convection regime (196 points), where both natural convection and nucleate boiling contribute to the heat transfer in the liquid pool, to within ±15% (Fig. 13).

As shown in Fig. 13, equation (13) provides a

smooth and continuous transition among all three heat transfer regimes in small liquid pools. Figure 13 also shows that the heat transfer data for uniformly heated, small liquid pools in cylindrical enclosures can effectively be classified into the different heat transfer regimes through the use of a dimensionless parameter, X , which is defined as:

$$X = \psi Ra^{0.35} Pr_1^{0.35} (p_l/\sigma)^{0.7} (q_c l_m / \rho_g h_{fg} v_l)^{0.7} \tag{14}$$

For natural convection, $X < 10^6$, for nucleate boiling

$X > 2.1 \times 10^7$, and in the intermediate regime of combined convection, $10^6 \leq X \leq 2.1 \times 10^7$. Figure 14 compares the present heat transfer correlations for all three regimes of natural convection, combined convection and nucleate boiling with the entire data base. As delineated in the figure, the present correlations are in good agreement with most data, to within $\pm 15\%$.

SUMMARY AND CONCLUSIONS

A total of 731 heat transfer data points for uniformly heated, small liquid pools in cylindrical enclosures were compiled, sorted and correlated in the different heat transfer regimes, namely: (a) natural convection (208 data points), at low heat fluxes; (b) nucleate boiling heat transfer (327 data points), at high heat fluxes; and (c) the intermediate regime of combined convection (196 data points). The compiled experimental data base covered a wide range of inner pool diameters (6–37 mm), heated pool heights (50–800 mm), working fluid filling ratios (0.1–3.25), and wall heat fluxes (0.7–383 kW m⁻²).

The natural convection data were correlated in terms of the liquid Rayleigh number in the pool [equation (10)], and the ratio of the bubble length scale to the inner diameter of the pool, (l_m/d_i), indicating the important contribution of bubble nucleation at the wall to the heat transfer in this regime. The nucleate boiling heat transfer data were correlated [equation (11)] in terms of the nucleate boiling heat transfer coefficient of Kutatelatze [2], and the mixing coefficient, ψ [equation (12a)], which accounts for the effect of mixing at the wall by sliding bubble and in the pool by large departing and rising bubbles. The mixing coefficient in the present nucleate boiling correlation [equation (11)], depends on the physical properties and operating vapor pressure of the working fluid [equation (12a)].

The proper selection of the dimensionless groups in the natural convection and nucleate boiling correlations have contributed to the good agreement of the present correlations with most data to within $\pm 15\%$. The data in the intermediate regime of combined convection were correlated by superimposing the correlations for natural convection and nucleate boiling using a power law approach [equation (13)]. The combined convection correlation was also within $\pm 15\%$ of most data (Table 1) and presented a smooth transition between all three heat transfer regimes.

Acknowledgements—This research is partially funded by the University of New Mexico's Institute for Space Nuclear Power Studies and the Egyptian Authority for Scientific Missions, Cairo, Arab Republic of Egypt.

REFERENCES

1. Foster, H. K. and Zuber, N., Dynamics of vapor bubbles and boiling heat transfer. *A.I.Ch.E. Journal*, 1955, **1**, 531.
2. Kutatelatze, S. S., *Heat Transfer in Condensation and Boiling*. AEC-tr-3770, 1959, p. 129.
3. Rohsenow, W. M., A method of correlating heat transfer data for surface boiling of liquids. *Transactions of the ASME*, 1962, **84**, 969.
4. Stephen, K. and Abdelsalam, M., Heat-transfer correlations for natural convection boiling. *International Journal of Heat and Mass Transfer*, 1980, **23**, 73–87.
5. Kusuda, H. and Imura, H., Boiling heat transfer in an open thermosyphon. *Bulletin of JSME*, 1973, **16**, 1734–1740.
6. Imura, H., Kusuda, H., Ogata, Jun-Ichi, Miyazki, T. and Sakamoto, N., Heat transfer in two-phase closed-type thermosyphons. *Journal of Heat Transfer Japanese Research*, 1979, **8**(2), 41–53.
7. Shiraiishi, M., Kikuchi, K. and Yamanishi, T., Investigation of heat transfer characteristics of a two-phase closed thermosyphon. *Proceedings of the 4th International Heat Pipe Conference*, London, U.K., Advances in Heat Pipe Technology, ed. D. A. Reay. Pergamon Press, New York, 1981, pp. 95–104.
8. Ueda, H., Miyashita, T. and Chu, Ping-hsu, Heat transport characteristics of a closed two-phase thermosyphon. *Transactions of the JSME, Series B*, 1988, **54**(506), 2848–2855.
9. Kaminaga, F., Okamoto, Y. and Suzuki, T., Study on boiling heat transfer correlation in a closed two-phase thermosyphon. *Proceedings of the 8th International Heat Pipe Conference*, Beijing, China, ed. Ma Tongze. Institute of Engineering Thermophysics, Chinese Academy of Sciences, 1992, pp. 317–322.
10. Groß, U., Pool boiling heat transfer inside a two-phase thermosyphon correlation of experimental data. *Proceedings of the 9th International Heat Transfer Conference*, Jerusalem, Israel, 1-Bo-10, 1990, pp. 57–62.
11. Jialun, H., Tongze, Ma and Zhengfang, Z., Investigation of boiling liquid pool height of a two-phase closed thermosyphon. *Proceedings of the 8th International Heat Pipe Conference*, Beijing, China, ed. Ma Tongze. Institute of Engineering Thermophysics, Chinese Academy of Sciences, 1992, pp. 154–159.
12. Churchill, S. W., A comprehensive correlating equation for laminar, assisting, forced and free convection. *A.I.Ch.E. Journal*, 1977, **23**(10), 10–16.
13. Cooper, M. G., Heat transfer in saturated nucleate pool boiling. *Advances in Heat Transfer*, 1984, **16**, 157–239.
14. Ruckenstein, E., Interpolating equations between two limiting cases for the heat transfer coefficient. *A.I.Ch.E. Journal*, 1978, **24**, 940–941.
15. El-Genk, M. S., Su, B. and Guo, Z., Experimental studies of forced, combined, and natural convection of water in vertical nine-rod bundles with a square lattice. *International Journal of Heat and Mass Transfer*, 1993, **36**(9), 2359–2374.
16. El-Genk, M. S., Bedrose, S. D. and Rao, D. V., Forced and combined convection of water in a vertical seven-rod bundle with $P/D = 1.38$. *International Journal of Heat and Mass Transfer*, 1990, **33**(6), 1289–1297.
17. El-Genk, M. S. and Rao, D., Heat transfer experiments and correlations for low Reynolds number flows of water in a vertical annuli. *International Journal of Heat and Mass Transfer*, 1989, **10**(2), 44–57.
18. Bezrodnyi, M. K. and Alekseenko, D. V., Boiling heat transfer in closed two-phase thermosyphons. *Izv. Vuzav, Energetika*, 1976, **12**, 96–101.
19. Xiang-Qun, C., Zhengfang, Z. and Tongze, Ma, Heat transfer correlation of the evaporator section in a two-phase closed thermosyphon. *Proceedings of the 8th International Heat Pipe Conference*, Beijing, China, ed. Ma Tongze. Institute of Engineering Thermophysics, Chinese Academy of Sciences, 1992, pp. 354–359.
20. Suematsu, H., Harada, K., Inoue, S., Fujita, J. and Wakiyama, Y., Heat transfer characteristics of heat

- pipes. *Heat Transfer—Japanese Research*, 1978, 7(1), 1–22.
21. Xin, M., Chen, G. and Chen, Y., Flow and heat transfer in two-phase closed thermosyphon. *Proceedings of the 6th International Heat Pipe Conference*, Grenoble, France, Vol. 3, 1987, pp. 419–423.
 22. Bezrodnyi, M. K. and Aleksenko, D. V., The intensity of heat transfer in boiling section of evaporator thermosyphons. *Teploenergetika*, 1977, 24(7), 83–85.
 23. Fujii, M., Boiling heat transfer of a two-phase closed thermosyphon with a porous surface. *Proceedings of the 5th International Heat Pipe Conference*, Tokyo, Japan, Vol. 2, 1984, pp. 105–111.